Adaptive chicken swarm optimization algorithm for identifying structural parameters of 6-DOF mechanical arm

Zhiqiang Xu (xzq17852674990@163.com)
Hubei University of Technology https://orcid.org/0000-0002-5439-037X
Junyong Xia
Hubei University of Technology
Fei Zhong
Hubei University of Technology

Research Article

Keywords: 6-DOF mechanical arm, structural parameters, single-point conical hole repeatability experiment, adaptability, chicken swarm optimization algorithm

Posted Date: July 6th, 2023

DOI: https://doi.org/10.21203/rs.3.rs-2975065/v1

Adaptive chicken swarm optimization algorithm for identifying structural parameters of 6-DOF mechanical arm

Xu Zhiqiang, Xia Junyong, Zhong Fei
(School of Mechanical Engineering, Hubei University of Technology, Wuhan Hubei 430068, China)
Xu Zhiqiang, e-mail: xzq17852674990@163.com, ORCID: 0000-0002-5439-037X

Abstract

Accurately identifying the structural parameters of the mechanical arm can effectively increase its precision. Firstly, the kinematic model of the mechanical arm is constructed by adopting the MDH method. Secondly, based on the single-point conical hole repeatability, the objective function characterizing the single-point repeatability error is established. Thirdly, an adaptive chicken swarm optimization algorithm (mCSO) is put forward to tackle the issue of low convergence accuracy of chicken swarm optimization algorithm (CSO). Then, combined with the objective function characterizing the single-point repeatability error, the structural parameters of the mechanical arm are identified using algorithms CSO and mCSO, respectively. Finally, repeat the single-point conical hole repeatability experiment using the mechanical arm before and after identification. The experimental result reveals that the single-point repeatability error of the mechanical arm after mCSO identification is greatly reduced.

Key words: 6-DOF mechanical arm; structural parameters; single-point conical hole repeatability experiment; adaptability; chicken swarm optimization algorithm

1 Introduction

Coordinate measuring machine (CMM) [1-2] can not only detect the size, shape, and mutual position of components such as boxes, tracks, turbines, cylinders, and gears, but also integrate lithography circuits and continuous surface scanning. However, when using CMM, the measured object can only be taken to the fixed CMM for measurement, which makes it unable to measure the object of specific industrial areas. So, based on the fact that CMM cannot meet many practical application requirements, the multiple-joint mechanical arm [3-4] has emerged. It imitates the physical structure of human hands and connects the links, probes, bases, and other components into a whole mechanism through a series of rotating joints. Its birth has largely addressed the measurement needs of objects in specific industrial areas. However, due to factors such as pressure, and wear in industrial areas, the structural parameters of the mechanical arm may change after a period of use. Because the impact of structural parameter errors on measurement results is nonlinear [5-6], tiny errors in certain structural parameters may lead to observable errors in the measurement results. Consequently, periodically identifying the structural parameters of the mechanical arm is indispensable.

At present, numerous researchers have made many attempts and works in identifying the structural parameters. Furutani et al. [7] used metal plates with multiple

standard balls to identify the structural parameters of the mechanical arm. Santolaria et al. [8] employed a ball club and self-centering detection technology to identify the structural parameters of the mechanical arm. Santolaria et al. [9] made use of spherical gauges and established an error model based on Fourier polynomials to identify the parameters of the mechanical arm. Kamali et al. [10] utilized a laser tracker to simultaneously identify the structural and stiffness parameters of the mechanical arm. Wang et al. [11] analyzed the relative pose relationship of adjacent links and created a specific identification ball based on this analysis, and then used the least squares method to identify the structural parameters. Liu et al. [12] identified the structural parameters of the mechanical arm by adopting the orthogonal coordinate measuring machine. Sun [13] used an electronic theodolite to identify the structural parameters of the mechanical arm.

It can be seen that although there are a variety of approaches to identify the structural parameters of the mechanical arm, most of these methods rely on precise components. And these components not only have expensive processing costs, but also have complex operating procedures and easy sensitivity to the environment. Therefore, a novel means coupling the single-point conical hole repeatability experiment and intelligent optimization algorithm is brought up to identify the structural parameters of the mechanical arm. Firstly, insert the probe end of the mechanical arm into the fixed conical hole on the platform. Secondly, shake the joints of the mechanical arm to various positions to change the joint angles, so as to obtain data on multiple sets of joint angles of the same point. Thirdly, identify the structural parameters of the mechanical arm using CSO and mCSO based on the collected data. Finally, repeat the single-point conical hole repeatability experiment using the mechanical arm before and after identification, and draw the conclusion.

2 Establishment of kinematic model and objective function

2.1 Establishment of kinematic model

The mechanical arm used in this article is shown in Fig 1.

Fig 1. Mechanical structure of the mechanical arm

The kinematic model is built to attain the transfer function between the coordinate

of the probe end and the structural parameters. The most commonly used modeling methods for the 6-DOF mechanical arm are the DH modeling method [14-15] and the MDH modeling method [16-17]. DH model is widely used in the mathematical modeling of the mechanical arm because of its clear physical meaning and simple mathematical structure. However, although this classic model has strong applicability, it also has its own shortcomings: for links with parallel or nearly parallel relationships, there are some singularities of the mechanical arm. Therefore, to prevent the occurrence of singularities, the MDH model is employed as the mathematical model of the mechanical arm.

The coordinate system of the mechanical arm is established according to the MDH rule, as shown in Fig 2. According to the principle of homogeneous coordinate transformation, the relative pose relationship between link $i-1$ and link i can be described by translation and rotation transformations.

$$T_{i-1,i} = R_X\left(\alpha_{i-1}\right) D_X\left(a_{i-1}\right) R_Z\left(\theta_i\right) D_Z\left(d_i\right) = \begin{bmatrix} cos\theta_i & sin\theta_i & 0 & a_{i-1} \\ sin\theta_i cos\alpha_{i-1} & cos\theta_i cos\alpha_{i-1} & -sin\alpha_{i-1} & d_i sin\alpha_{i-1} \\ sin\theta_i sin\alpha_{i-1} & cos\theta_i sin\alpha_{i-1} & cos\alpha_{i-1} & -d_i cos\alpha_{i-1} \\ 0 & 0 & 0 & 1 \end{bmatrix}. \tag{1}$$

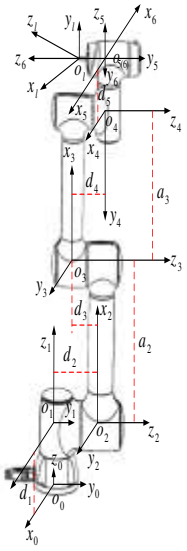

Fig 2. Coordinate figure of the mechanical arm

Where a_{i-1} is joint offset, α_{i-1} is joint torsion angle, d_i is link length, and θ_i is joint angle. When calculating the probe end's coordinate (x, y, z) in the base coordinate system $\{o_0 x_0 y_0 z_0\}$, in addition to the four sets of structural parameters mentioned above, the coordinate of the probe (l_x, l_y, l_z) in the last joint coordinate system $\{o_6 x_6 y_6 z_6\}$, namely the probe offset, is also required. The probe offset is used as the fifth set of structural parameters of the mechanical arm.

$$\begin{bmatrix} x \\ y \\ z \\ 1 \end{bmatrix} = T_{0,1} \cdot T_{1,2} \cdot T_{2,3} \cdot T_{3,4} \cdot T_{4,5} \cdot T_{5,6} \cdot \begin{bmatrix} l_x \\ l_y \\ l_z \\ 1 \end{bmatrix} =$$

$$\prod_{i=1}^{6} \begin{bmatrix} cos\theta_i & sin\theta_i & 0 & a_{i-1} \\ sin\theta_i cos\alpha_{i-1} & cos\theta_i cos\alpha_{i-1} & -sin\alpha_{i-1} & d_i sin\alpha_{i-1} \\ sin\theta_i sin\alpha_{i-1} & cos\theta_i sin\alpha_{i-1} & cos\alpha_{i-1} & -d_i cos\alpha_{i-1} \\ 0 & 0 & 0 & 1 \end{bmatrix} \cdot \begin{bmatrix} l_x \\ l_y \\ l_z \\ 1 \end{bmatrix}. \tag{2}$$

In addition, errors during assembly often cause the misalignment of the encoder's physical zero position and the joint zero position [9]. Thus, the joint zero position's deviation $\theta_{0,i}$ and the angle sensor reading $\theta_{s,j}$ constitute the joint angle θ_i. And $\theta_{s,j}$ is a variable that can be directly read. Hence, the five sets of structural parameters identified in this article are shown in Table 1.

$$\theta_i = \theta_{0,i} + \theta_{s,j}. \tag{3}$$

Table 1 Structural parameters of the mechanical arm

Joint number	a_{i-1} /mm	α_{i-1} /°	d_i /mm	$\theta_{0,i}$ /°	Probe offset (mm)
1	0	0	147.5	0	$l_x = 0$
2	0	-90	156	0	
3	395	0	112	0	$l_y = 0$
4	375	0	127.5	0	
5	0	-90	130	0	$l_z = 47$
6	0	90	0	0	

2.2 Establishment of objective function

To vectorize the structural parameters, set $X = (a_0, a_1, a_2, a_3, a_4, a_5, \alpha_0, \alpha_1, \alpha_2, \alpha_3, \alpha_4, \alpha_5, d_1, d_2, d_3, d_4, d_5, d_6, \theta_{0,1}, \theta_{0,2}, \theta_{0,3}, \theta_{0,4}, \theta_{0,5}, \theta_{0,6}, l_x, l_y, l_z)$. According to equations (2) and (3), probe end's coordinate of the mechanical arm can be written as a function of structural parameter X and angle sensor reading $\theta_{s,j}$.

$$\begin{bmatrix} x \\ y \\ z \end{bmatrix} = \begin{bmatrix} f_x\left(\theta_{s,1}, \theta_{s,2}, \theta_{s,3}, \theta_{s,4}, \theta_{s,5}, \theta_{s,6}, X\right) \\ f_y\left(\theta_{s,1}, \theta_{s,2}, \theta_{s,3}, \theta_{s,4}, \theta_{s,5}, \theta_{s,6}, X\right) \\ f_z\left(\theta_{s,1}, \theta_{s,2}, \theta_{s,3}, \theta_{s,4}, \theta_{s,5}, \theta_{s,6}, X\right) \end{bmatrix}. \tag{4}$$

Specifically, If the probe end's coordinates in N positions can be acquired by instruments with higher accuracy. And combining the N sets of coordinate values and corresponding joint angles, $3N$ equations can be derived from equation (4). Then, by extracting these $3N$ equations, the actual structural parameters of the mechanical arm can be obtained. However, these $3N$ equations are implicit equations and difficult to gain its solution. Therefore, this paper puts forward a single-point conical hole repeatability experiment to identify the structural parameters of the mechanical arm. According to single-point conical hole repeatability experiment mentioned above, the site is shown in Fig 3. Firstly, insert the probe end into the fixed conical hole on the platform. Secondly, shake the joints of the mechanical arm to N different positions and postures to acquire N sets of joint angles ${}^k\theta_{s,i}\left(i = 1, 2, \ldots, 6; k = 1, 2, \ldots, N\right)$ about the same point. Then, For any set of structural parameter X and collected N sets of

joint angles ${}^{k}\theta_{s,i}\left(i=1,2,\ldots,6;k=1,2,\ldots,N\right)$, the error between the probe end's coordinate $({}^{k}x,{}^{k}y,{}^{k}z)(k=1,2,...,N)$ and the probe end's actual coordinates $(x_{mean},y_{mean},z_{mean})$ can be expressed by Equation (5).

$$ {}^{k}E=\sqrt{({}^{k}x-x_{mean})^{2}+({}^{k}y-y_{mean})^{2}+({}^{k}z-z_{mean})^{2}}. \tag{5}$$

(a)Global figure (b)Partial figure

Fig 3. Test Site of single-point conical hole repeatability experiment

Nevertheless, the fact is that the probe end's actual coordinate is difficult to be acquired, so the average of N sets of the probe end's coordinates $({}^{k}x,{}^{k}y,{}^{k}z)$ is used to replace the actual coordinate, i.e.

$$\begin{cases} x_{mean}=\dfrac{1}{N}\displaystyle\sum_{i=1}^{N}{}^{k}x \\ y_{mean}=\dfrac{1}{N}\displaystyle\sum_{i=1}^{N}{}^{k}y. \\ z_{mean}=\dfrac{1}{N}\displaystyle\sum_{i=1}^{N}{}^{k}z \end{cases} \tag{6}$$

To indicate the single-point repeatability error of the mechanical arm, the mean and standard deviation of ${}^{k}E$ are employed to establish the objective function (9).

$$\bar{E}=\frac{1}{N}\sum_{k=1}^{N}{}^{k}E. \tag{7}$$

$$\sigma=\sqrt{\frac{1}{N-1}-\sum_{i}^{N}({}^{k}E-\bar{E})^{2}}. \tag{8}$$

$$F\left(X\right)=\bar{E}+3\sigma. \tag{9}$$

Obviously, the structural parameter X is closer to the actual structural parameter, the objective function value is smaller. Assuming X^{*} is the actual structural parameter, then the objective function value is 0. Based on this, the next task is to combine intelligent optimization algorithms to find X^{*} or infinitely approaching the solution of X^{*}.

3 Adaptive Chicken Swarm Optimization Algorithm

3.1 Basic Chicken Swarm Optimization Algorithm

Meng et al. [18] developed CSO in 2014. Firstly, CSO assigns the role of each chicken according to its fitness value. The rooster has the strongest adaptability and a

leading advantage. The number of hens is the largest, mainly learning from the rooster. The chick has the weakest adaptability, following their mother and conducting local searches around her. Secondly, the entire chicken herd is partitioned into multiple families, and each family is composed of a rooster, a number of hens, and a few of chicks. Then, owing to difference of the roles, the rooster, the hen, and the chick need different kinds of motion to take on their own responsibilities.

The motion equation of the rooster is as follows:

$$X_{i,j}(t+1) = X_{i,j}(t) \times \left(1 + randn\left(0, \sigma^2\right)\right). \tag{10}$$

$$\sigma^2 = \begin{cases} 1, f_i \le f_k \\ exp\left(\dfrac{f_k - f_i}{|f_i| + \varepsilon}\right), f_i > f_k \end{cases}. \tag{11}$$

Where $X_{i,j}(t)$ means the position of the $j-th$ dimension of rooster i in the $t-th$ iteration. $randn\left(0,\sigma^2\right)$ stands for a Gaussian distribution with mean 0 and standard deviation σ. ε is a minimal non-zero constant, ensuring that the denominator is not zero. k is a randomly selected rooster and $k \neq i$. f is the individual's fitness value.

The motion equation of the hen is as follows:

$$X_{i,j}(t+1) = X_{i,j}(t) + C_1 \times rand \times \left(X_{r1,j}(t) - X_{i,j}(t)\right) + C_2 \times rand \times \left(X_{r2,j}(t) - X_{i,j}(t)\right). \tag{12}$$

$$C_1 = \exp\left(\frac{f_i - f_i}{|f_i| + \varepsilon}\right). \tag{13}$$

$$C_2 = \exp\left(f_{r2} - f_i\right). \tag{14}$$

Where i is a hen. $rand$ refers to a random number on 0-1. r_1 indicates the rooster in the subgroup of the $i-th$ hen. $r_2\left(r_2 \neq r_1\right)$ is randomly selected from the entire population, requiring $f\left(Xr_2\right) > f\left(X_i\right)$.

The motion equation of the chick is as follows:

$$X_{i,j}(t+1) = X_{i,j}(t) + FL \times \left(X_{m,j}(t) - X_{i,j}(t)\right). \tag{15}$$

Where i is a chick. m is mother of the $i-th$ chick. And $FL\left(FL \in [0,2]\right)$ is a parameter called the following coefficient.

With the iterative operation of the algorithm, the fitness value of each chicken has changed differently, so the structure of the subgroup should also be adjusted accordingly. Therefore, to adapt to this change, parameter G was introduced. G is a special parameter in CSO, which determines the speed of population evolution. Numerous studies have found that when the value of G is [2,20] [18], most optimization problems can be tackled.

3.2 Adaptive Chicken Swarm Optimization Algorithm

3.2.1 inertia weight

The inertia weight strategy can dynamically and adaptively regulate the weights of the individual self-learning and global learning to transform their moving steps. So, to enhance the dynamic adaptive ability of each chicken, suppress the attenuation of population diversity, and increase the accuracy of the solution, two inertial weights are

introduced into CSO. To visually demonstrate the characteristics of the inertia weights, equations (16) and (17) provide their functions, and Fig 4. shows their image.

$$w_1 = \sin(\frac{\pi}{2} \times \frac{t}{\max gen}). \tag{16}$$

$$w_2 = \cos(\frac{\pi}{2} \times \frac{t}{\max gen}). \tag{17}$$

Where t is the current iteration and $\max gen$ is the maximum number of iterations.

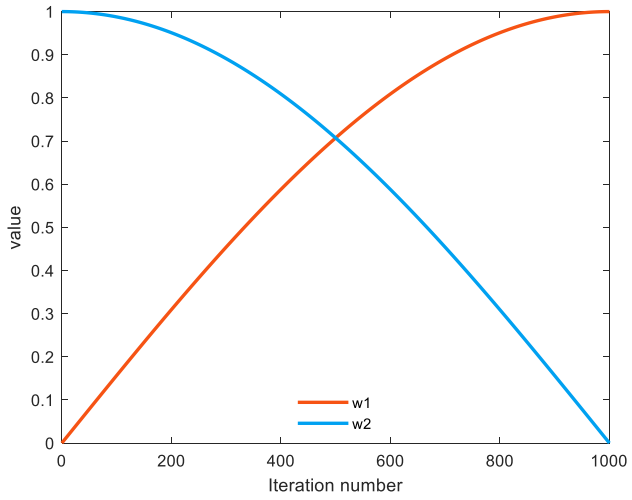

Fig 4. Inertial weight image

3.2.2 Improved rooster's motion equation

In basic CSO, a random learning strategy based on Gaussian distribution is applied to the motion equation of the rooster. This learning strategy can give the rooster an edge in local search ability, but it will bring inferiorities to the rooster's global search [19]. In other words, the rooster is prone to falling into local optima. Once the rooster gets stuck at locally optimal value, strict hierarchical system is also highly likely to cause the hen and the chick to trap in local optima. Therefore, considering that the rooster needs to lead their subgroups to globally optimize in unknown environments, they should optimize in a wider area. So, the improved rooster's motion equation is as follows. Firstly, the rooster not only needs to learn from itself, but also from the optimal individual $X_{best,j}(t)$. Secondly, introduce inertia weights w_1 and w_2 into the modified equation. The specific functions of the two inertia weights are as follows. In the initial iteration of the algorithm, the optimal individual is essential to the immature rooster. This means that the rooster's fitness value can be rapidly improved and can move towards the optimal solution by w_2. As the algorithm runs, most roosters will gradually approach $X_{best,j}(t)$. To avoid premature convergence of the algorithm, the self-information of each rooster is more utilized by continuously increasing w_1 and gradually decreasing w_2..

$$X_{i,j}(t+1) = w_1 \times X_{i,j}(t) + w_2 \times \left(X_{best,j}(t) - X_{i,j}(t)\right). \tag{18}$$

3.2.3 Improved hen's motion equation

Although the hen does not have the leading advantage of the rooster, as the most numerous individuals in a subgroup, they also play a considerable role in optimizing.

As a result, nonlinear inertia weight w_2 and the optimal solution $\mathrm{X}_{best,j}(t)$ are added to the motion equation of the hen.

$$X_{i,j}(t+1)=w_2\times X_{i,j}(t)+\mathrm{C}_1\times\mathrm{rand}\times\left(X_{r1,j}(\mathrm{t})-X_{i,j}(t)\right)+\mathrm{C}_2\times\mathrm{rand}\times\left(\mathrm{X}_{best,j}(\mathrm{t})-X_{i,j}(t)\right). \tag{19}$$

$$C_2=\exp\left(f_{best}-f_i\right). \tag{20}$$

3.2.4 Improved chick's motion equation

Similarly, w_2 is also introduced to adjust the weight of self-learning and learning from the mother.

$$X_{i,j}(t+1)=w_2\times X_{i,j}(t)+FL\times\left(X_{m,j}(t)-X_{i,j}(t)\right). \tag{21}$$

3.3 Steps of mCSO

Step 1: Initialize the parameters and the chickens' position.

Step 2: Calculate the fitness of each chicken, and record the optimal fitness value and its corresponding individual.

Step 3: If it is $mod(iter,G)=1$, sort the fitness values of the chickens and divide them into different subgroups.

Step 4: Update the position of the rooster on the basis of equation (18).

Step 5: Update the position of the hen according to equations (13), (19), and (20).

Step 6: Update the position of the chick using equation (21).

Step 7: Judge $iter \geq \max gen$. If so, the algorithm will terminate. Otherwise, the algorithm will proceed to step 2.

4 Result analysis

Based on the collected joint angle data, CSO and mCSO is used to identify the structural parameters of the mechanical arm. To provide a fair and unbiased identification process, The number of chickens in both CSO and mCSO is 100, and the proportion of roosters, hens, and chicks is 2:6:2. G takes 10, and the iteration limit is 5000. In addition, calculation operation of the algorithm may give rise to the structural parameters to cross the corresponding boundary values. So, Table 2 lists the boundary values of structural parameters.

Table 2 Boundary values of structural parameters

Joint number	a_{i-1}/mm	α_{i-1}/°	d_i/mm	$\theta_{0,i}$/°	Probe offset (mm)
1	0~10	-10~10	137.5~157.5	-1~1	$l_x=-10\sim10$
2	0~10	-100~-80	146~166	-1~1	
3	385~405	-10~10	102~122	-1~1	$l_y=-10\sim10$
4	365~385	-10~10	117.5~137.5	-1~1	
5	0~10	-100~-80	120~140	-1~1	$l_z=37\sim57$
6	0~10	80~100	0~10	-1~1	

For the convenience of comparison, when CSO and mCSO identify the structural parameters of the mechanical arm, the objective function's evolution curve is drawn in a coordinate system, as shown in Fig 5. Tables 3 and 4 separately summarize the structural parameters of the mechanical arm optimized by two sets of algorithms. After attaining two sets of optimized structural parameters, they are independently transmitted to the controller as new structural parameters of the mechanical arm. Then, single-point conical hole repeatability experiment is conducted using the mechanical arm before identification, after CSO identification, and after mCSO identification,

respectively. And Fig 6. draw the single-point repeatability error curves of the mechanical arm before identification, after CSO identification, and after mCSO identification. Table 5 provides the single-point repeatability error before identification, after CSO identification, and after mCSO identification. Tables 6, 7, and 8 individually offers the components of the single-point repeatability error in the three coordinate axis directions. By analyzing and comparing the above results, it is not difficult to see that the single-point repeatability error and its corresponding components in the three coordinate axis directions of the mechanical arm after mCSO identification have significantly decreased.

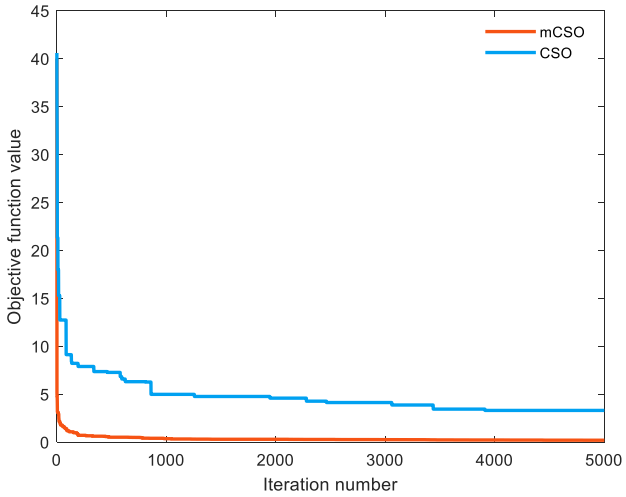

Fig 5. Objective function evolution curve of CSO and mCSO

Table 3 Structural parameters of the mechanical arm after CSO identification

Joint number	a_{i-1} /mm	α_{i-1} /°	d_i /mm	$\theta_{0,i}$ /°	Probe offset (mm)
1	0.2286	0.1776	147.4468	0.0846	l_x =0.3721
2	0.0843	-89.6327	156.7291	0.0331	
3	395.5861	-0.3084	112.0538	0.1726	l_y = 0.4984
4	374.9637	0.9227	127.7508	-0.0722	
5	0.4625	-90.3372	129.5949	-0.0186	l_z = 46.4146
6	0.0837	90.1397	0.1184	0.0508	

Table 4 Structural parameters of the mechanical arm after mCSO identification

Joint number	a_{i-1} /mm	α_{i-1} /°	d_i /mm	$\theta_{0,i}$ /°	Probe offset (mm)
1	0.2442	0.1362	147.5298	-0.0653	l_x =0.2561
2	0.0746	-89.5672	155.7053	0.0347	
3	394.7592	-0.2475	112.0732	0.0846	l_y = -0.3631
4	375.1278	0.9373	127.2984	-0.1063	
5	0.2431	-90.2335	129.6743	-0.0492	l_z = 47.6286
6	0.0745	90.1989	0.0977	0.0274	

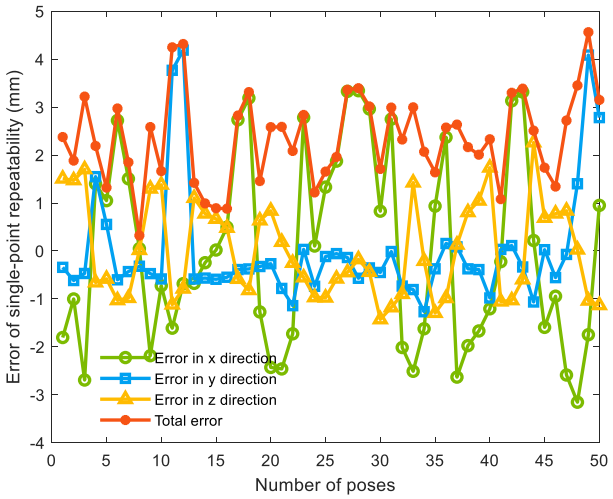

(a) Single-point repeatability error curve before identification

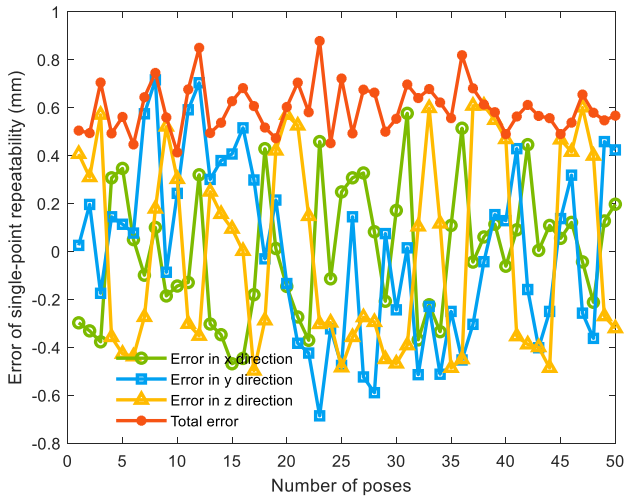

(b)Single-point repeatability error curve after CSO identification

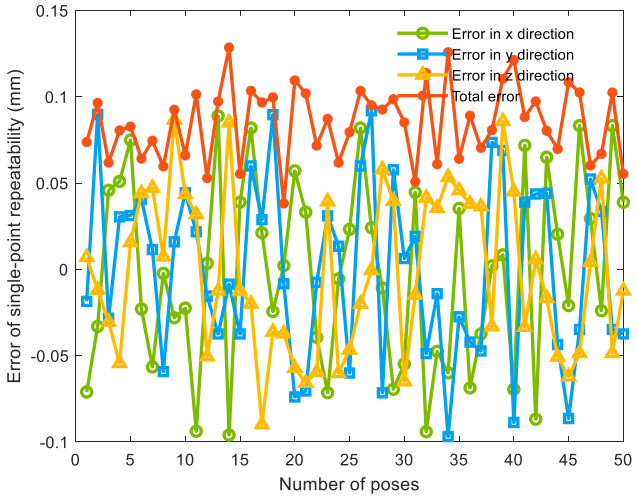

(c) Single-point repeatability error curve after mCSO identification

Fig 6. Single-point repeatability error curve

Table 5 Error of single-point repeatability before, after CSO identification, and after mCSO identification

	Maximum /mm	minimum /mm	mean/mm	std/mm
Before identification	4.5633	0.3231	2.3626	0.9325
After CSO identification	0.8785	0.4139	0.5983	0.1024
After mCSO identification	0.1285	0.0382	0.0846	0.0212

Table 6 x direction error of single-point repeatability before identification, after CSO identification, and after mCSO identification

	Maximum /mm	minimum /mm	mean/mm	std/mm
Before identification	3.3424	0.0193	1.7357	2.0173
After CSO identification	0.5768	0.0048	0.2278	0.2735
After mCSO identification	-0.0960	0.0020	0.0464	0.0547

Table 7 y direction error of single-point repeatability before identification, after CSO identification, and after mCSO identification

	Maximum /mm	minimum /mm	mean/mm	std/mm
Before identification	4.1893	-0.0119	0.7510	1.2247
After CSO identification	0.7165	0.0157	0.3118	0.3680
After mCSO identification	-0.0968	0.0063	0.0440	0.0511

Table 8 z direction error of single-point repeatability before identification, after CSO identification, and after mCSO identification

	Maximum /mm	minimum /mm	mean/mm	std/mm
Before identification	2.2623	0.0173	0.8722	0.9980
After CSO identification	0.6089	0.0025	0.3759	0.4069
After mCSO identification	-0.0898	-0.0005	0.0400	0.0463

5 Conclusion

Firstly, although CSO has the positives of dynamically updating subgroups and

simultaneously evolving multiple subgroups, it has defects of low convergence accuracy when solving the complicated problem. In response to the deficiency, mCSO is put forward. Secondly, due to the fact that most of the existing methods for identifying the structural parameters of the mechanical arm rely on high-precision equipment, a new method combining mCSO and the single-point conical hole repeatability experiment is raised to identify the structural parameters of the mechanical arm. Finally, after comparative analysis of relevant experiments, the following conclusions can be drawn. It is almost unrealistic to solve the actual structural parameters of the mechanical arm. The structural parameters optimized by mCSO can greatly reduce the single-point repeatability error of the mechanical arm. And in fact, the identification method presented in this article can bring much convenience to the structural parameter identification of mechanical arm in industrial sites.

Funding and Conflicts of interests

This work was supported by Wuhan Science and Technology Achievements Transformation Project (No.2020030603012342)

The authors have no competing interests to declare that are relevant to the content of this article.

References

[1] CHEN H F, SUN M Y, GAO Y, et al. A method for solving geometric errors of large CMMs using elastic network algorithm [J]. China Mechanical Engineering, 2022, 33(09):1077-1083 (in Chinese).

[2] ZENG B ZHOU Y S, WANG S H, et al. Tooth profile error measurement of face gear based on universal CMM [J]. Journal of Aerodynamics, 2022, 37(04):856-868(in Chinese).

[3] BRAN A, VALENZUELA M, SANTOLARIA J, et al. Evaluation of different probing systems used in articulated arm coordinate measuring machines [J]. Polska Akad Nauk, Polish Acad Sciences, 2014, 21(2): 233-246.

[4] JOUBAIR A, SLAMANI M, BONEV IA. A novel XY-Theta precision table and a geometric procedure for its kinematic calibration [J]. Pergamon-Elsebier Science Ltd, 2012, 28(1): 57-65.

[5] El ASMAI S, HENNEBELLE F, COOREVITS T, et al. Rapid and robust on-site evaluation of articulated arm coordinate measuring machine performance [J]. Measurement Science and Technology, 2018, 29(11).

[6] OSTROWSKA K, GASKA A, KUPIEC R, et al. Comparison of accuracy of virtual articulated arm coordinate measuring machine based on different metrological models [J]. Measurement, 2019, 133: 262-270.

[7] FURUTANI R, SHIMOJIMA K TAKAMASU K. Parameter calibration for non-cartesian CMM [J]. Measure and Quality Control in Production, 2004,1860: 317-326.

[8] SANTOLARIA J, BRAU A, VELZAQUEZ J, et al. A self-centering active probing technique for kinematic parameter identification and verification of articulated arm coordinate measuring machines [J]. Measurement Science and Technology, 2010, 21(5).

[9] SANTOLARIA J, AGUILAR JJ, YAGUE JA，et al. Kinematic parameter estimation technique for calibration and repeatability improvement of articulated arm coordinate measuring machines [J]. Precision Engineering，2008，32(4): 251-268.

[10] KAMALI K, JOUBAIR A, BONEV IA, et al. Elasto-geometrical calibration of an industrial robot under multidirectional external loads using a laser tracker [C] // Okamura A. 2016 IEEE International Conffrence on Robotics and Automation. New York: IEEE, 2016: 4320-4327.

[11] WEI L, WANG C J. Coordinate conversion and parameter calibration of multi joint coordinate measuring machines [J]. Photoelectric Engineering, 2007, (05):57-61(in Chinese).

[12] LIU W L, QU X H, YAN Y G. Calibration and error compensation of portable coordinate measuring arms [J]. Journal of Instrumentation, 2007，28(4): 81- 84(in Chinese).

[13] SUN H X, TAN Y S, JIA Q X, et al. Research on a new method for measuring the motion accuracy of manipulator based on electronic theodolite[J]. Journal of Instrumentation, 2007，28(12):2206- 2209(in Chinese).

[14] YANG JQ, WANG DY, FAN BX, et al. Online absolute pose compensation and steering control of industrial robot based on six degrees of freedom laser measurement [J]. Optical Engineering, 2017, 56(3).

[15] WANG LP, CHEN L, SHAO ZF, et al. Analysis of flexible supported industrial robot on terminal accuracy [J]. International Journal of Advanced Robotic Systems, 2018, 15(4).

[16] GAO GB, LI Y, LIU F, et al. Kinematic Calibration of Industrial Robots Based on Distance Information Using a Hybrid Identification Method [J]. Complexity, 2021.

[17] GAO G B, NIU J P, LIU F, et al. Positioning error compensation for 6-DOF robot based on anisotropic error similarity [J]. Optical Precision Engineering, 2022, 30(16):1955-1967(in Chinese).

[18] MENG XB, LIU Y, GAO XZ , et al. A new bio-inspired algorithm: chicken swarm optimization [C] // Tan Y. Lecture Notes in ArtifIcial Intelligence. Berlin: SpringerLink, 2014, 8794: 86-94.

[19] QU CW, ZHAO SA, Fu YM, et al. Chicken swarm optimization based on elite opposition-based learning [J]. Mathematical Problems in Engineering, 2017.

[20] Rao R V, Savsani V J, Vakharia D P. Teaching–learning-based optimization: A novel method for constrained mechanical design optimization problems [J]. Computer-Aided Design, 2011, 43(3): 303-315.

[21] NIE Y H, ZHANG C L, GAO Lei, et al. Parameter identification method of static var compensator model based on improved chicken swarm algorithm [J]. Power grid technology, 2019, 43(02):731-738(in Chinese).